

Specific Interactions of Sodium Salts with Alanine Dipeptide and Tetrapeptide in Water: Insights from Molecular Dynamics

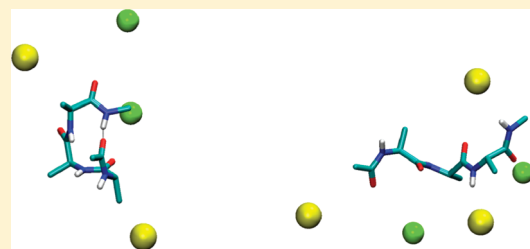
Filippos Ioannou,[†] Georgios Archontis,^{*,‡} and Epameinondas Leontidis^{*,†}

[†]Department of Chemistry, University of Cyprus, PO20537, Nicosia 1678, Cyprus

[‡]Department of Physics, University of Cyprus, PO20537, Nicosia 1678, Cyprus

 Supporting Information

ABSTRACT: We examine computationally the dipeptide and tetrapeptide of alanine in pure water and solutions of sodium chloride (NaCl) and iodide (NaI), with salt concentrations up to 3 M. Enhanced sampling of the configuration space is achieved by the replica exchange method. In agreement with other works, we observe preferential sodium interactions with the peptide carbonyl groups, which are enhanced in the NaI solutions due to the increased affinity of the less hydrophilic iodide anion for the peptide methyl side-chains and terminal blocking groups. These interactions have been associated with a decrease in the helicities of more complex peptides. In our simulations, both salts have a small effect on the dipeptide, but consistently stabilize the intramolecular hydrogen-bonding interactions and “ α -helical” conformations of the tetrapeptide. This behavior, and an analysis of the intermolecular interaction energies show that ion–peptide interactions, or changes in the peptide hydration due to salts, are not sufficient determining factors of the peptide conformational preferences. Additional simulations suggest that the observed stabilizing effect is not due to the employed force-field, and that it is maintained in short peptides but is reversed in longer peptides. Thus, the peptide conformational preferences are determined by an interplay of energetic and entropic factors, arising from the peptide sequence and length and the composition of the solution.



1. INTRODUCTION

The Hofmeister series, which orders small inorganic ions on the basis of their effects on protein solubility, has puzzled scientists for more than a century, but no general consensus has been reached about the exact mechanism of specific ion action.^{1–5} In the past few years, research on specific salt effects has been reinvigorated by the advent of powerful new experimental and computational methodologies. Regarding computations, new ideas about salt effects have been tested with the advent of improved additive or polarizable force fields.^{6–8} New insights have been obtained, resulting in a large increase of scientific work on the origin of specific ion action at aqueous interfaces.^{5,9,10} The contribution of porizability to the attraction of loosely hydrated ions to the free water surface, hydrophobic or hydrophilic self-assembled monolayers, or lipid bilayers has been investigated.^{9,11–16}

Despite these recent advances, much less progress has been made in understanding salt effects on protein stability and solubility that would open up new vistas for biology and enzymology. It is thus surprising that this scientific area, which initially triggered the research on ionic specificity, is currently the least advanced. Current research in this area follows two main directions: On one hand there are workers that try to understand the specific interactions of ions with protein surfaces,^{17,18} (either direct or water-mediated^{19,20}) or the salt-mediated protein–protein interactions and the second virial coefficients of protein solutions.²¹ These researchers address the problem of protein solubility and

crystallization from solution, and the surface-mediated mechanisms of salting-in and salting-out. A different line of investigation, originally carried out experimentally^{22–26} but more recently and to a larger extent computationally,^{27–33} is the use of specially designed oligopeptides and other related model compounds^{32,34} in the effort to assess the specific ionic interactions with the peptide backbone or with individual side chains, and the effects of ions on the secondary structure of the peptides. These works address more directly the issue of protein stability and conformation.

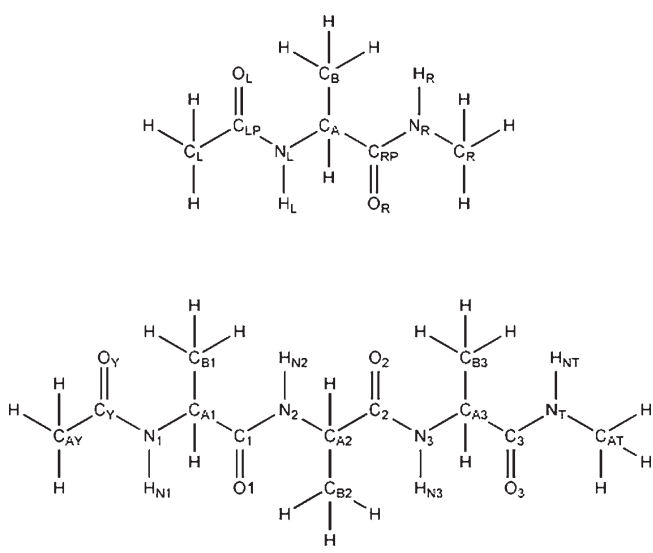
Our present work falls in this second group. Here we have carried out a systematic investigation of specific ion effects on alanine dipeptide and tetrapeptide aqueous solutions, in an effort to obtain the necessary information to answer the following questions: (a) Do ions have a measurable impact on the preference of oligopeptides for special conformations *in solution*? If yes, how are these conformations stabilized/destabilized? Can one identify specific interactions with side groups or with the backbone that play major roles in the stabilization process? (b) Do ions have a measurable impact on the preference of the bare protein backbone for certain secondary structure elements, as manifested in Ramachandran plots of a simple dipeptide?³⁵ (c) How do the ions affect the hydration of the peptides? Is the

Received: July 25, 2011

Revised: October 5, 2011

Published: October 06, 2011

Scheme 1. Terminally Blocked Alanine Dipeptide (Ac-Ala-NMe) and Tetrapeptide (Ac-Ala₃-NMe) Used in the Present Investigation



competition of ions and peptides for water clearly seen in simulations?

Question (a) examines the impact of solvent on short- and long-range interactions, which are present in oligopeptide chains (and proteins), and ultimately determine the thermodynamically important conformations. Numerous theoretical studies have focused on short oligoalanine peptides, which serve as models of peptide conformation dynamics and helix formation.^{25,29,30,37–39} A detailed mapping of interactions is sought here, examining not only radial distribution functions (rdf's) at the pair-interaction level,^{27–31} but also the ensemble of possible conformations, and the nature of those that are enhanced or “destroyed” by the presence of electrolytes. In this respect, our analysis is related to the recent work of Dzubiella on alanine-based peptides^{29,30} or that of Fedorov et al.,^{27,28} but we carry out a detailed analysis of all intermolecular interactions to identify potential driving forces for the observed conformational changes in the presence of salts. The discussion about specific ionic interactions with various groups on peptides and protein surfaces has been going on for a long time.^{1–3,32,34,39–45} It is not clear, however, how these binding interactions may affect the overall conformation of an oligopeptide.

Question (b) is fundamentally important. Even though an oligopeptide is not a protein, and a protein helix is typically stabilized by a variety of long-range interactions that are not present in the case of short peptides,^{35,36} a noticeable ionic effect on the Ramachandran plot of simple oligopeptides could have a significant effect on large protein structures as well, even though in ref 39 it was argued that local residue interactions do not determine sequence-dependent torsional preferences of peptide backbones. To the best of our knowledge, very few similar investigations have appeared to date,^{25,29–33} and the question is still under intense investigation. Two other recent papers examined the interactions between ions and n-methyl acetamide (NMA), the simplest model compound of the peptide bond.^{32,34} Finally, question (c) is also fundamental since many researchers currently believe that ionic specificity at interfaces stems from the competition between water and ions for interfacial sites or

from the competition of ions and the surface for water of hydration.^{5,46–49} Does a similar balance exist in salt solutions of oligopeptides, which also compete with ions for water of hydration? This is an issue, which, in our opinion, has not been closely examined in the recent simulation works, which focus mostly on ion-peptide interactions.^{27–32}

In this investigation we have opted to avoid direct charge interactions, since we are more interested in the specific interactions of ions with neutral (polar and nonpolar groups), and in the effect of the salt on the hydration of the peptide. We have therefore used the simplest possible oligopeptides: the properly blocked alanine dipeptide (Ac-Ala-NMe)^{49–52} and alanine tetrapeptide (Ac-(Ala)₃-NMe).⁵³ The chemical structures of the two molecules and the atom nomenclature are shown in Scheme 1. The alanine dipeptide serves as a model of the protein backbone (excluding the backbone moieties of glycine and proline residues), and has been extensively used in the optimization of peptide and protein empirical force fields.⁵⁴ It has a single pair of backbone dihedral angles (φ, ψ) and two peptide groups, which can form an intramolecular hydrogen bond. It allows checking the specific ion effects on the Ramachandran plot and the relative interaction of the ions with the backbone peptide groups and the methyl side chain and blocking groups.^{49–52}

The tetrapeptide introduces additional dimensions.⁵³ With the present choice of N-terminal and C-terminal blocking groups, it has three complete pairs of backbone torsional angles (φ_i, ψ_i) and four peptide groups. Thus, it can form a variety of hydrogen-bonding interactions, including two $i/i+3$ hydrogen bonds encountered in β -turns ($C_Y O_Y - N_3 H_{N_3}$, $C_1 O_1 - N_T H_{N_T}$; Scheme 1), and one $i/i+4$ hydrogen bond encountered in α -helices ($C_Y O_Y - N_T H_{N_T}$). Thus, closed, “quasi-helical” conformations are now possible, and the conformational space is greatly extended with respect to the dipeptide. Even though no large-scale secondary structure can be formed by the tetrapeptide, an increase of “closed” conformations would immediately signify that the presence of salts stabilizes the initial helix-formation step in this type of oligopeptides.

To keep the systems simple, we have only used sodium chloride (NaCl) and sodium iodide (NaI) as electrolytes. NaCl is generally expected not to give strong specific salt effects in most systems,^{1,2,5,47} while iodide is definitely a chaotropic anion and can be used to illustrate potential side-chain or backbone interactions of the more hydrophobic ions.^{27–30} We have used a range of electrolyte concentrations (0–3 M) to investigate concentration effects on the oligopeptide structures.

The accurate sampling of electrolyte solutions requires long simulation times. To accelerate sampling, we have used the powerful replica exchange simulation method, which simultaneously propagates several replicas of the system at various temperatures and allows the controlled exchange of conformations between different temperatures.^{55,56}

The result of the present work is a reasonably complete mapping of specific salt effects on the conformational preferences of the alanine dipeptide and tetrapeptide. These insights will be used as a starting point to understand salt effects on longer oligopeptides, for which the development of secondary structure is possible.

2. METHODS

2.1. Investigated Systems. The peptides studied have the sequences Ac-Ala-NMe and Ac-Ala₃-NMe (Scheme 1), with

Table 1. Numbers of Ions and Water Box Sizes Employed in the Simulations

solution	# waters	# cations	# anions	box length (Å)
Alanine Dipeptide				
0 M	1000	0	0	31.05
1.2 M NaCl	1000	22	22	31.33
2.3 M NaCl	1000	44	44	31.55
1.2 M NaI	1000	22	22	31.33
2.3 M NaI	1000	44	44	31.55
Alanine Tetrapeptide				
0 M	1000	0	0	31.05
1.2 M NaCl	1000	22	22	31.33
2.3 M NaCl	1000	44	44	31.55
3.1 M NaCl	1000	60	60	31.80
1.2 M NaI	1000	22	22	31.33
2.3 M NaI	1000	44	44	31.55
3.1 M NaI	1000	60	60	31.80

$C_LH_3C_{LP}O_L$ —(Ac) and $-N_RH_RC_RH_3$ (NMe), respectively, as the N- and C-terminal blocking groups. Each simulation system consisted of a single dipeptide or tetrapeptide molecule in a cubic box of 1000 water molecules and an appropriate number of ions, chosen to model the desired salt concentration. Table 1 lists the total number of ions and water-box sizes for the various dipeptide and tetrapeptide simulations. Although the actual salt concentrations are those listed in the table, for simplicity we will designate them as “1 M”, “2 M” or “3 M” concentrations in the ensuing discussion.

2.2. Force Field and Simulation Protocol. The peptide atomic charges, van der Waals, and stereochemical parameters were taken from the CHARMM22 all-atom force field,⁵⁷ including a recent grid-based torsional (CMAP) correction.^{58,59} The water was represented by a modified TIP3P model.^{60,61} Ion parameters, recently optimized for high-concentration simulations, were taken from Joung and Cheatham.⁶²

Simulations with short alanine-based peptides and comparisons with available experimental data suggest that several of the current biomolecular forcefields, including the CHARMM22/CMAP forcefield employed here, tend to overestimate the α -helical section of the Ramachandran map, at the expense of extended (β -sheet and PPII) conformations.^{25,37,63–66} This overstabilization is likely to have a smaller impact on the conformational preferences of the very short peptides considered here. Furthermore, the main goal of the present work is to monitor the dependence of conformational properties on salt type and concentration. Even if the helical propensities are systematically overestimated, the errors are likely to partially cancel in the propensity changes (among solutions). To check the force-field dependence of our observations, we also simulated the same alanine tetrapeptide, a nonapeptide (Ace-Ala₉-NMe), and a hexadecapeptide (Ace-(AQAAA)₃-NMe) in pure water and a 3.0 M NaI aqueous solution, using AMBER11⁶⁷ and the all-atom AMBER force field, with recent optimizations (ff03*) improving peptide helicity at 300 K.⁶⁴ The main conclusions of the simulations with these two peptides and their relevance to the present work are presented in the Results section; details will be supplied in a forthcoming publication.

All other simulations were conducted with the CHARMM program,⁶⁸ version c35b3. The simulation system was replicated by cubic periodic conditions, using the CRYSTAL facility of CHARMM. Electrostatic interactions were calculated by the particle-mesh Ewald method,⁶⁹ with a parameter $\kappa = 0.55555$ for the charge screening and sixth-order splines for the mesh interpolations. Lennard-Jones interactions between atom pairs were switched to zero for distances larger than 9 Å.⁶² The lengths of covalent bonds involving hydrogen atoms and the internal water molecule geometries were constrained to standard values via the SHAKE algorithm⁷⁰ implemented in CHARMM.

All solutions were studied by the replica-exchange molecular dynamics method.^{55,56} Simulations were performed in the canonical ensemble (N, V, T), with all atoms explicitly represented. Nosé-Hoover dynamics^{71,72} was conducted, using a 50.0 kcal/mol sec² thermal inertia parameter (QREF) and a 2 fs time step. For each solution, we used 18 replicas with temperatures 290, 295, 300, 305, 310, 315, 321, 327, 333, 339, 345, 351, 358, 365, 372, 379, 386, and 393 K. The NaCl solutions were initially equilibrated by constant pressure simulations at 300 K. Subsequently, the box sizes were fixed to the average size of the constant-pressure runs; identical box sizes were used for NaCl and NaI solutions of the same concentration. The replica temperatures were then optimized by serial, constant volume simulations, targeting an exchange acceptance probability between adjacent replicas of ~20%. The obtained exchange-probabilities were between 16 and 21%. All replicas performed random walks in the temperature space, spanning several times the entire range of temperatures; for example, in a typical tetrapeptide solution, the temperature space was traversed ~26 times during a 25 ns simulation. The total simulation length at each temperature was 20 ns for the dipeptide (360 ns for each solution) and 25 ns for the tetrapeptide (450 ns for each solution). Exchanges between adjacent replicas were attempted every 500 steps (1 ps). The last 19 ns (dipeptide) or 20 ns (tetrapeptide) were employed in the analysis.

2.3. Secondary Structure Calculations and Conformational Analysis. We computed the tetrapeptide “helicity” (the fraction of α -helical conformations), using the Lifson-Roig (LR) model.⁷³ In the LR definition, a residue i is considered α -helical if and only if its backbone torsional angles (φ_i, ψ_i), and the pairs ($\varphi_{i-1}, \psi_{i-1}$) and ($\varphi_{i+1}, \psi_{i+1}$) of the adjacent residues fall in the α -helical region of the Ramachandran map ($\varphi = -65 \pm 35^\circ$, $\psi = -37 \pm 30^\circ$). Since the tetrapeptide has three torsional angle pairs, a conformation was classified as α -helical if and only if all three torsional angle pairs were simultaneously in the α -helical region.

The alanine tetrapeptide can also form two β turns, respectively involving the atom pairs $C_YO_Y-N_3HN_3$ and $C_1O_1-N_TH_{NT}$ (see Scheme 1). A β -turn was considered present if the following criteria of Wilmut and Thornton⁷⁴ applied: (i) the distance $C_{\alpha,i}-C_{\alpha,i+3}$ was smaller than 7 Å, (ii) the torsional angles of residues $i+1$ and $i+2$ were not in the helical region of the Ramachandran map, and (iii) the torsional angles of residues $i+1$, and $i+2$ were within $\pm 30^\circ$ of the ideal turn values,⁷⁴ with one dihedral allowed to deviate by $\pm 45^\circ$. For the first and second β -turn, we used, respectively, the N-terminal methyl carbon (CAY) or the C-terminal methyl carbon (CAT) in criterion (i). Note that criterion (ii) implies that a β -turn cannot coexist with the α -helical state. Main-chain hydrogen bonds were considered present if the distance between the carbonyl oxygen and the amino hydrogen was less than 2.5 Å, without considering any additional angle restrictions.

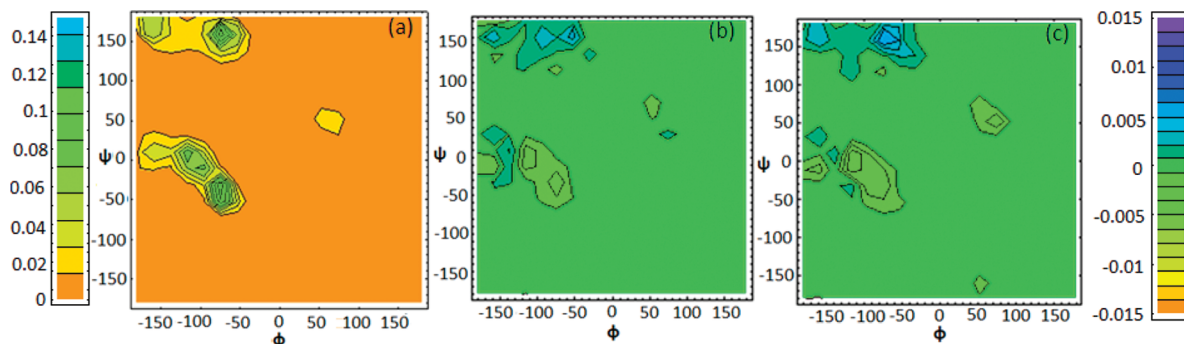


Figure 1. (a) Joint probability density map of the dipeptide torsional angle pair (ϕ, ψ) in pure water; the associated color-code is on the leftmost panel. (b,c) Change in probability when pure water is replaced by a 2 M NaCl solution or a 2 M NaI solution, respectively. The rightmost color-code refers to the last two plots. All maps correspond to 300 K.

We classified the tetrapeptide conformations into families, using conformational clustering of the six backbone torsional angles.^{75–77} The clustering method is presented in detail in ref 76. Briefly, a trajectory snapshot j is described by a set of K predetermined properties (here backbone torsional angles), arranged into a K -dimensional vector $\vec{x}_j = (x_{1j}, x_{2j}, \dots, x_{Kj})$. The center of a cluster l containing $M(l)$ snapshots is defined by the arithmetic mean $c_l = (c_{1l}, c_{2l}, \dots, c_{Kl}) \equiv 1/M(l)\sum_{j \in M(l)} \vec{x}_j$. Each of the $M(l)$ snapshots comprising cluster l is within a certain predefined threshold (radius) d_0 from the cluster center c_l (i.e., $[\sum_{i=1}^K (x_{il} - c_{il})^2]^{1/2} \leq d_0$). The maximum cluster radius was set to 50° , corresponding to average structural fluctuations of approximately 20° for each of the six torsional angles.

3. RESULTS

3.1. Alanine Dipeptide Simulations. Figure 1a displays the joint probability distribution of the dipeptide main-chain torsional angles from the no-salt simulations at 300 K. The preferred backbone conformations (yellow to green areas) fall mainly into the extended- β region ($\phi = -160 \pm 10^\circ$, $\psi = 170 \pm 10^\circ$), the PPII region ($\phi = -75 \pm 15^\circ$, $\psi = 160 \pm 20^\circ$), and a broad, right-handed α -helical basin with two subregions ($\phi = -70 \pm 20^\circ$, $\psi = -60 \pm 20^\circ$ and $\phi = -115 \pm 30^\circ$, $\psi = 0 \pm 20^\circ$).³⁴ A small fraction of left-handed α -helical conformations is also observed ($\phi = 65 \pm 15^\circ$, $\psi = 50 \pm 10^\circ$). The distribution agrees very well with the map of ref 56, which was also obtained with the CHARMM22⁵⁷ force-field and the grid-based correction (CMAP).^{58,59} As shown in that work, this distribution reproduces reasonably well the statistics from Protein Data Bank (PDB)-deposited protein conformations, as well as quantum mechanics/molecular mechanics (QM/MM) calculations.⁷⁸ However, compared to available spectroscopic data for the alanine dipeptide in solution, which report a propensity of the peptide for the PP-II conformation,^{79–81} the present forcefield clearly favors the α -helical region.

The addition of 2 M NaCl or 2 M NaI to the system does not lead to dramatic changes of the main chain torsional angle probability distribution, as shown in the difference plots (electrolyte solution vs pure water) of Figure 1b,c. A slight stabilization of polyproline II conformations is observed for both salts, more so for the chaotropic NaI. Nevertheless, we can state that the dipeptide conformations are weakly affected by electrolytes, at least within the confines of the forcefield that we used.^{57–59} A related observation was made by Feig, who investigated effects of

sequences on backbone torsional preferences, by simulations with several dipeptides and proteins.³⁹ Such effects were not apparent in the dipeptide models, but required longer-range interactions, encountered in the context of larger polypeptide chains and protein structures. As we show below, electrolytes have a much more significant impact on the conformational properties of the tetrapeptide.

In the ensuing discussion, we refer to the “left” (L) side of the dipeptide as the one closer to the N-terminal end, and to the “right” (R) side as the one closer to the C-terminal end. The rdf's between selected pairs of electrolyte ions and peptide atoms are shown in Figure 2; they correspond to simulations at 300 K. The Na^+ – $\text{O}_{\text{L/R}}$ rdf curves (Figure 2a) have a pronounced first-contact peak (~ 4), reflecting the strong sodium interactions with the peptide carbonyl groups. Contrary to this, the larger anion (I^-) has a stronger affinity for the dipeptide amide groups relative to the smaller anion (Cl^-), as reflected by the first contact peaks of the corresponding rdf's with the amide hydrogens $\text{H}_{\text{L/R}}$ (Figure 2b). Both first-contact peaks are, however, below unity, reflecting the lack of preference for the bulkier anions to interact directly with the peptide groups. This behavior of cations and anions is well documented in simulations of model peptides in salt solutions.^{29,32}

Anions in both NaCl and NaI solutions interact more strongly with H_{R} (Figure 2b). This preference might be related to the significant difference of solvent accessible areas of the two amide groups (11.1 \AA^2 for N_{R} vs 6.3 \AA^2 for N_{L}). By contrast, Na^+ ions in NaCl solutions appear to interact more weakly with the C-terminal peptide oxygen (O_{R}), compared to the N-terminal peptide oxygen (O_{L}) (Figure 2a); this is probably within the simulation uncertainty, since the two groups have comparable solvent accessible areas (33.1 \AA^2 for O_{R} vs 35.9 \AA^2 for O_{L}).

I^- has a stronger propensity than Cl^- to approach the nonpolar side-chain and blocking methyl groups (Figure 2c). The first solvation peaks of the rdf's between iodide ions and nonpolar methyl groups (Figure 2c) are actually larger than unity, illustrating a preferential interaction, while the corresponding chloride–C peaks are much smaller than unity, showing that chloride ions avoid the hydrophobic methyl groups. This behavior of iodide has been observed in other simulations of oligopeptide electrolyte solutions;^{27–29} it is partly due to the larger radius of the iodide first hydration shell, which facilitates the loss of hydration water around iodide, relative to chloride. Overall, the dipeptide results show that ions affect to a small extent the intrinsic conformation tendencies of the backbone,

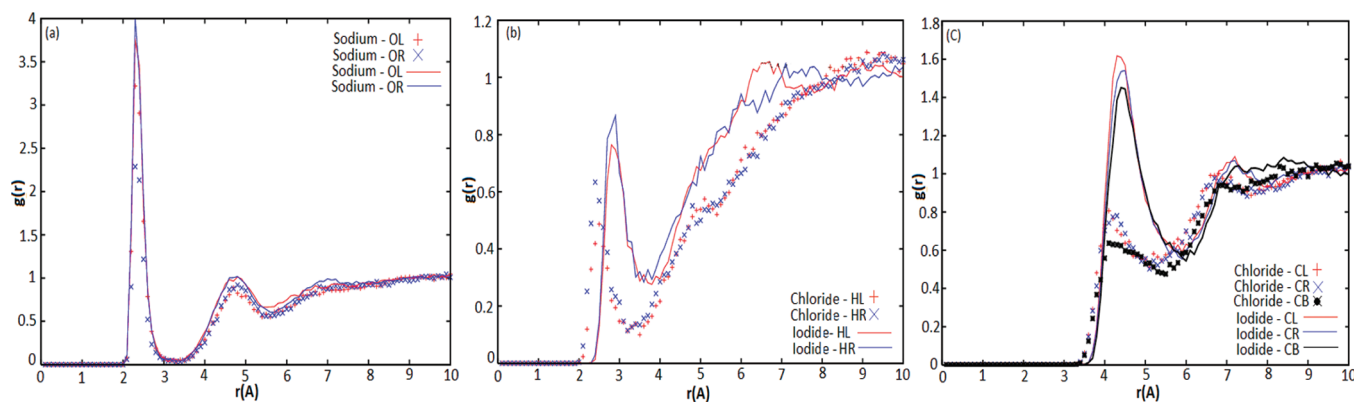


Figure 2. Radial distribution functions (RDFs) between selected ion–dipeptide atom pairs (at 300 K). (a) sodium–carbonyl oxygen; (b) anion–amino-group hydrogen; (c) anion–methyl carbon. “L” and “R” denote atoms in the “left” (N-terminal) and “right” (C-terminal) groups; “CB” is the side chain atom (Scheme 1). In all plots, lines correspond to the 2 M NaI solution, and symbols correspond to the 2 M NaCl solution.

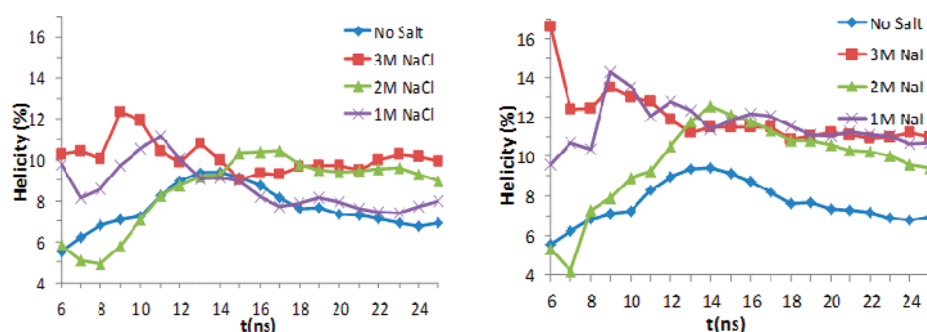


Figure 3. Cumulative average helicity of the alanine tetrapeptide, plotted versus simulation time in (a) NaCl and (b) NaI solutions of various concentrations; pure-water results are also included.

and that larger anions interact more strongly with the hydrophobic regions of the chain, in accordance with previous investigations of similar systems.^{27–29}

3.2. Tetrapeptide Simulations. As explained in the Methods section, the employed tetrapeptide model can form an elementary α -helix, one $i/i+4$ hydrogen bond, and two $i/i+3$ hydrogen bonds. In the classification of α -helical conformations, we used the LR convention,⁷³ which requires all three main-chain torsional angle pairs to fall in the α -helical region of the Ramachandran map (Methods).

Figure 3 displays cumulative averages of the resulting “helicities” (fractions of α -helical conformations), at 300 K, with respect to simulation length. The helicities converge slowly toward time-independent averages, because they are proportional to the joint probabilities of all three angle pairs; nevertheless, the limiting values demonstrate certain consistent trends: The helical conformations are stabilized in all electrolyte solutions, relative to pure water. Even in the least well-equilibrated samples (2 M NaCl and 2 M NaI solutions) the limiting helicity values are much higher than the corresponding value of the pure-water case, strongly supporting the conclusion that salts enhance helicity. Such differences are unlikely to disappear by prolonging the simulation.

The cumulative average helicity in pure water was found roughly equal to 7%. This is reasonable, given our definition of average helicity, which requires all three residues to be in a helical conformation simultaneously. In the literature experimental values of 20% for the second from the N-terminal alanine residue

and 10% for the third from the N-terminal residue of tetraalanine have been measured using a combination of spectroscopic methods.^{82,83} Older simulation work has also concluded that the helical conformation of the trialanine may be less than 10%,⁸⁴ although experiment suggests values closer to 20%.⁸³

Even though the average helicities decrease (almost linearly) with temperature, this stabilization persists in the entire temperature range (290–390 K) of the simulations. This is shown in Figure S1 of the Supporting Information (SI), which displays the temperature dependence of average helicities. Near 300 K, the helicities increase with salt concentration; beyond ~ 320 K, they become independent of electrolyte type and concentration.

Recent simulations with more complex oligopeptides suggest a complex dependence of helical stability on salt. In the case of the negatively charged alanine-based peptide Ac-(AE)₆-NMe, examined with the Amber ff03 force-field, a significant reduction in α -helix content in the presence of NaI³⁰ and a slight increase in other solutions (NaCl, KCl, KI) were reported.³⁰ This behavior was mainly attributed to enhanced sodium interactions with the peptide carbonyl groups in the presence of iodide, due to the affinity of the latter for the hydrophobic Ala side chains. In the case of the positively charged peptide [Ac-(AK)₆-NMe], NaI had no effect on the helix, whereas the chloride salts NaCl and KCl stabilized it.³⁰ Another study, also with Amber ff03, considered the peptide Ace-AEAAAKEAAKA-NMe. The chosen sequence contains oppositely charged side-chains at positions $i/i+4$, which can form salt-bridge interactions in an α -helical conformation. Simulations in high electrolyte concentrations (3–4 M) suggested a small

Table 2. Average Helicities and Hydrogen-Bond Probabilities (%) for the Ala Tetrapeptide Solutions^a

system	helicity (%)	hydrogen bond (%)			total hydrogen bond probability (%)
		<i>i, i+4</i>	<i>i, i+3</i>	<i>i, i+2</i>	
Pure Water	6.9 ± 3.1	7.8 ± 3.4	6.8 ± 2.2	5.2 ± 1.2	19.8 ± 5.5
1 M NaCl	8.0 ± 2.0	9.3 ± 1.8	7.2 ± 1.6	5.8 ± 0.7	22.3 ± 5.5
2 M NaCl	9.0 ± 3.1	10.0 ± 2.9	9.0 ± 1.6	6.9 ± 1.5	25.9 ± 5.8
3 M NaCl	9.9 ± 2.6	11.7 ± 3.3	9.3 ± 1.9	7.1 ± 0.5	28.1 ± 5.1
1 M NaI	10.7 ± 2.0	11.3 ± 1.6	8.6 ± 0.5	6.9 ± 0.2	26.8 ± 2.8
2 M NaI	9.4 ± 4.1	10.7 ± 3.4	9.3 ± 1.9	5.5 ± 0.8	25.5 ± 6.8
3 M NaI	11.0 ± 1.4	12.1 ± 1.7	9.5 ± 1.5	5.6 ± 0.8	27.2 ± 3.7

^a The results are averaged over the last 20 ns of the simulations; standard deviations are computed by separating the trajectories into four blocks of 5 ns.

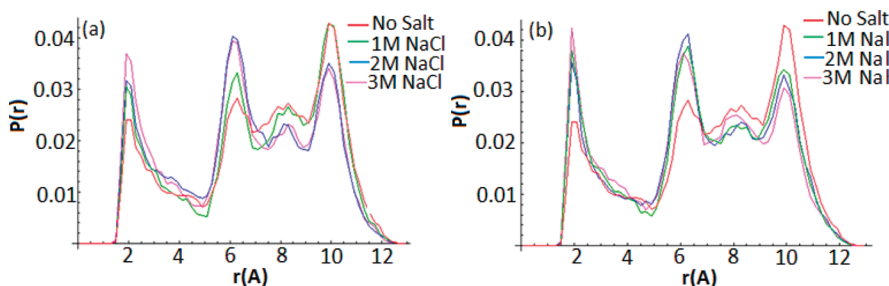


Figure 4. Histograms of the tetrapeptide terminal atom pair distance OY – HNT for (a) NaCl solutions, and (b) NaI solutions. The pure-water histogram is also included in both diagrams as a reference.

destabilization of the α -helix in the presence of NaCl, and a larger destabilization in the presence of NaI.²⁹ This destabilization was attributed to a combined effect, due to screening of the salt-bridge interactions by the salt, and enhanced sodium–carbonyl interactions in the presence of iodide. In a different study by Asciutti et al. with the Amber ffSB99 force-field, the helicity of a charged alanine-based 21-residue peptide with three arginine residues was shown to increase in the presence of NaClO₄.³¹

Those studies and the present work suggest that the peptide conformational stability is determined by a complex balance of energetic and entropic factors, which depend on the solution (salt type and concentration), the peptide composition, and its length. The peptides of our study have simpler sequences and significantly shorter lengths, compared to the systems of refs 29–31. We also observe enhanced iodide affinities for the side chain and terminal blocking methyl groups, and pronounced sodium–carbonyl interactions in the presence of iodide, both in the dipeptide (Figure 2a) and the tetrapeptide (below) solutions. These interactions have only a small impact on the dipeptide conformation, as demonstrated by the small changes in the torsional angle probability maps (Figure 2), presumably due to the small size of this system. In the case of the tetrapeptide, the enhanced interactions are accompanied by an *increase* in the α -helix population. An intermediate Ala oligopeptide with charged terminal ends (NH_3^+ -Ala₃-COO⁻) was studied in aqueous solutions of sodium halide salts by Fedorov et al.,^{27,28} using the OPLSAA-2001 force field⁸⁵ in Gromacs⁸⁶ and a TIPSP-EW⁸⁷ water model; the observed conformations depended on salt concentration and type, with high electrolyte concentrations usually favoring extended conformations. Thus, the above-mentioned ion–peptide interactions alone cannot determine the conformational preferences of these model peptides.

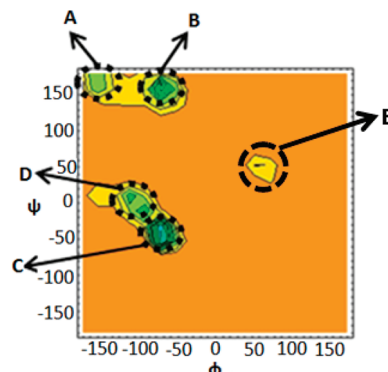


Figure 5. Ramachandran map, displaying the probability distribution of the tetrapeptide main-chain torsional angles ϕ , ψ in pure water at 300 K; the probability is averaged over the three torsional pairs. Color code is as in Figure 1a.

Apart from the sequence and the composition of the solution, the simulation conformational properties of a peptide depend on the employed force fields. The CHARMM force field employed here is known to overstabilize helical conformations in peptides.^{25,37,63–66} To investigate the extent of force-field dependencies in our results, we performed additional simulations with a recently modified version of the Amber all-atom force field (ff03*),⁶⁴ which reproduces the experimentally observed helical population of short, alanine-based peptides at 300 K. The water TIP3P model^{60,61} and ion parameters⁶² were the same as in the CHARMM calculations. The resulting tetrapeptide helicities in pure water and a 3 M NaI solution were too low ($\sim 2\text{--}3\%$), to draw conclusions. We therefore studied the longer peptides Ace-Ala₈-NMe (Alanine nonapeptide) and Ace-(AAQAA)₃-NMe

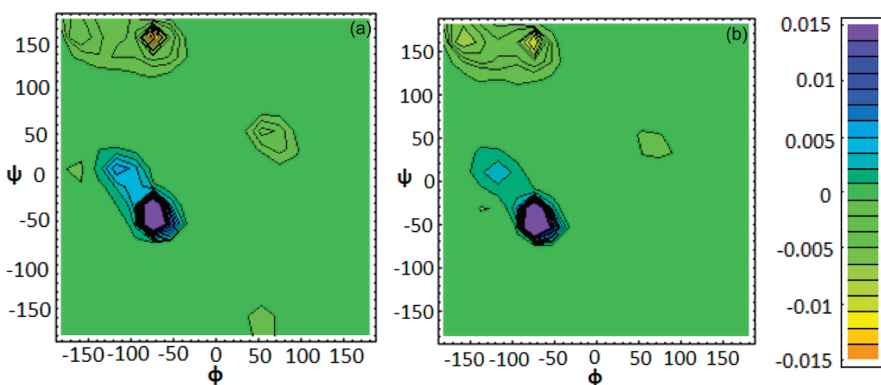


Figure 6. Difference (salt vs pure water) maps of the two-dimensional probabilities for the tetrapeptide main-chain torsional angles; the probabilities are averaged over the three torsional angle pairs: (a) 3 M NaCl solution; (b) 3 M NaI solution. A color code is provided.

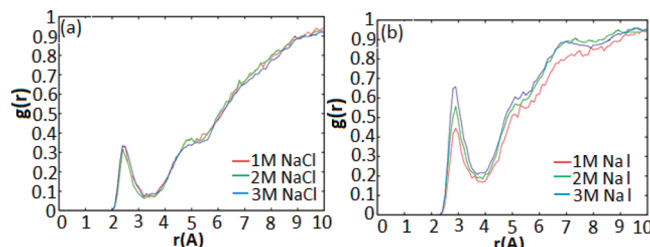


Figure 7. Anion–amide hydrogen rdf's for (a) NaCl solutions of various concentrations, and (b) NaI solutions of various concentrations.

(hexadecapeptide). A detailed presentation of the results will appear in a forthcoming paper, which examines salt effects on the conformational preferences of longer peptides. It suffices to state here that the nonapeptide helicity was increased in a 3 M NaI solution, relative to pure water (12.5% at 297 K, compared to 8.8%). This is in agreement with the prediction of the CHARMM22/CMAP^{27,58,59} force field for the (shorter) alanine tetrapeptide; by contrast, for the hexadecapeptide, the helicity was significantly decreased in a 3 M NaI solution, relative to pure water (11.6% and 18.7%, respectively, at 300 K). These results suggest that the helical stabilization by NaI is a more general phenomenon for *short* peptides, unrelated to the CHARMM force field. However, the same salt apparently destabilizes the helical conformation in longer peptides; additional comparisons of peptides with various lengths are needed to explain this result (work in progress).

To obtain more insights on the helical stabilization observed here, we summarize in Table 2 the average peptide helicities and hydrogen-bond occupancies at 300 K, for all solutions. As expected, the helicities are correlated with the probabilities of the α -helical ($i/i+4$) hydrogen-bond. Interestingly, the ions also cause a notable increase in the occupancies of other hydrogen-bonds. As with the helicity, this increase is monotonic with salt concentration in the NaCl solutions. Thus, the salts seem to promote the general stabilization of folded conformations for the tetrapeptide, via the strengthening of hydrogen-bonding interactions.

This is also shown in Figure 4, which displays distance histograms of the $i/i+4$ hydrogen-bonding atom pair O_Y–H_{NT}. There are four distinguishable peaks at 2.2, 6.2, 8.5, and 10 Å. The conformations corresponding to these four peaks are similar

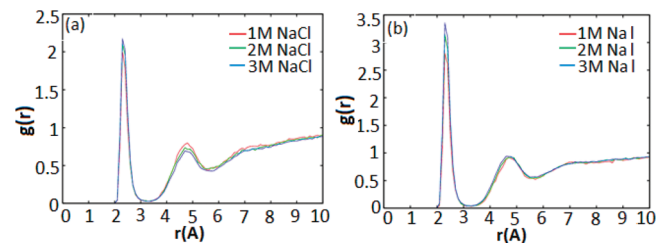


Figure 8. Sodium–carbonyl oxygen rdf's for (a) NaCl solutions and (b) NaI solutions.

across all solutions studied; in other words, we can state that in all solutions, peak 1 is mostly helical with some C_YO_Y–N₃H_{N3} β -turns, peak 2 has both β -turns, with C_YO_Y–N₃H_{N3} dominant, and so forth. Cluster analysis showed that the short-distance peak contains mainly helical conformations, or type-I β -turns involving the pair C_YO_Y – N₃H_{N3} (the respective probabilities are 77.5% and 15.4% in the 1 M NaCl solution). The peak at 6.2 Å contains mostly conformations with either type I β -turn, between C_YO_Y and N₃H_{N3} or C₁O₁ and N_TH_{NT} (respectively, 37.7% and 22.8% in 1 M NaCl). The broad peak around 8.5 Å and the peak at 10 Å contain extended conformations, without hydrogen bonds. In a fraction of the conformations contributing to these last two peaks, the main-chain dihedral angles adopt values near the PPII helix region. Table S1 in the electronic SI contains the detailed results of the peaks of Figure 4. The presence of salt causes an increase in the first two peaks and a decrease in the last two peaks, in agreement with the increase in hydrogen-bonded structures, reported in Table 2.

Figure 5 shows the joint probability distribution of the tetrapeptide backbone torsional angles in pure water, averaged over the three torsional angle pairs. The preferred conformations are found in five different regions of the Ramachandran plot, as in the case of the dipeptide (Figure 1a): regions A ($\phi = -160 \pm 10^\circ$, $\psi = 170 \pm 10^\circ$), B ($\phi = -75 \pm 15^\circ$, $\psi = 160 \pm 15^\circ$), C ($\phi = -75 \pm 15^\circ$, $\psi = -45 \pm 15^\circ$), D ($\phi = -110 \pm 15^\circ$, $\psi = 0 \pm 15^\circ$), and a less-occupied region E ($\phi = 65 \pm 15^\circ$, $\psi = 50 \pm 15^\circ$). While regions A and B correspond to extended peptide conformations (respectively, β -sheets and polyproline II in a protein), and C and D correspond to compact, folded peptide conformations (in a protein these would be right-handed α -helices), the less frequently occupied region E corresponds to left-handed helical conformations.³⁴

Figure 6 plots the corresponding probability differences (3 M electrolyte solution vs pure water), averaged over the three torsional angle pairs. The addition of NaCl causes a decrease of the probabilities in the extended conformation regions A and B, and an increase in the α -helical regions C and D. This behavior is in agreement with the increased tetrapeptide helicity in electrolyte solutions reported in Table 2. In the case of NaI, the increase of the probability maxima in regions C and D is more pronounced, in line with the larger observed helicity.

There appears to be a difference in the salt effects on internal dipeptide (increasing PP-II) and tetrapeptide (decreasing PP-II, increasing helical) conformations. This could be partly explained by the fact that the tetrapeptide can form three internal hydrogen bonds ($i/i+2, i/i+3, i/i+4$), compared to a single hydrogen bond ($i/i+2$) for the dipeptide; the occupancies of these bonds are increased by salt, promoting the helical conformations in the larger peptide (see Table 2).

To obtain microscopic insights about the observed helicity changes, we analyzed the various rdf's; selected functions are discussed below. The rdf curves of the anion (Cl^- or I^-)—amide pairs are displayed in Figure 7, averaged over the tetrapeptide amide groups. The contact peak of the chloride rdf is not sensitive to concentration and is in fact much lower than unity, showing that this anion is excluded from the vicinity of the amide group; this was also observed in the dipeptide simulations. In the case of iodide, the contact peaks are higher. Furthermore, all of the rdf curves (up to 10 Å) increase considerably with concentration. Thus, iodide interacts more strongly with the peptide group, and this interaction increases with salt concentration.

Sodium has a strong affinity for the peptide carbonyl groups as shown by the pronounced first solvation peaks of the corresponding rdf in Figure 8. This affinity is enhanced in NaI, relative to NaCl solutions. We believe that this is related to the higher simultaneous affinity of iodide for the peptide methyl groups, as also observed in the dipeptide simulations (Figure 2) and elsewhere.^{29,30,32} Nevertheless, it is accompanied by an increase in helicity for the tetrapeptide vs no effects for the dipeptide, reflecting the insufficiency of these interactions to account entirely for the conformational preferences of the peptide. This is further analyzed below.

Figure 9 displays the rdf functions between the anions and the side-chain methyl groups. As in the case of the dipeptide (Figure 2c), Cl^- actually avoids the methyl groups, and an increase in NaCl concentration does not enhance the weak interaction between Cl^- and the side chain carbon; I^- , on the contrary, has a stronger interaction with the methyl carbons, which increases with NaI concentration (the first rdf peaks are actually a little larger than unity, indicating a preference for the side group region by 0.1–0.2 kcal/mol). These findings are in agreement with the behavior of the anions toward the hydrophobic groups of the dipeptide (Figure 2c) and other works.^{27,29,30} Table S2 in the SI contains pair interaction energies between the ions, water, and various peptide groups.

An interesting question is whether the ions lead to dehydration of the peptide. This has been proposed as a plausible reason for the enhanced helicities in related systems.³⁰ To examine this question, in Figure 10 we compare the rdf's between water and the amide- or carbonyl groups in the presence of electrolytes. In all curves, the contact peaks are insensitive to the presence of ions. A small increase of the second solvation peak with salt concentration is observed (more clearly for NaI solutions), suggesting that the density of water at some distance from the

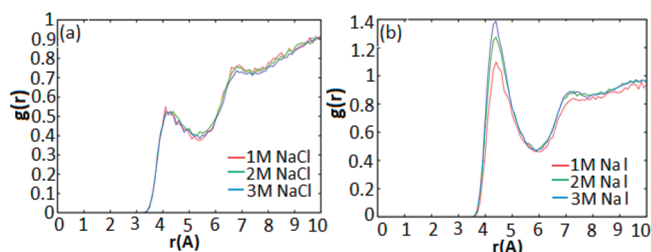


Figure 9. Anion—peptide side-chain methyl rdf's for (a) NaCl solutions and (b) NaI solutions.

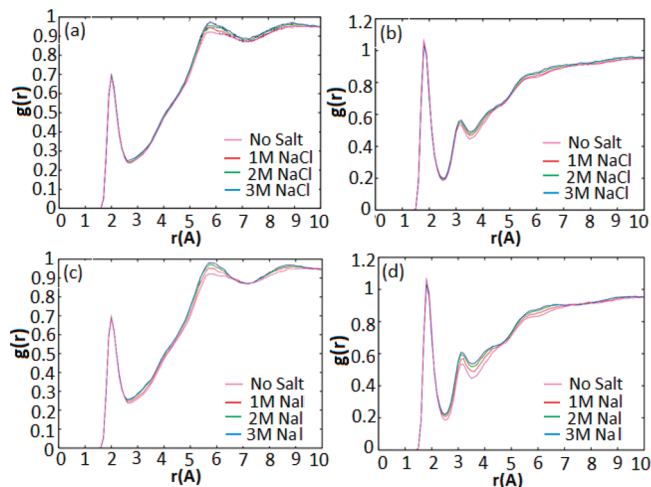


Figure 10. Peptide—water rdf's. (a,c) Water oxygen—amide hydrogens and (b,d) water hydrogen—carbonyl oxygens. Top plots: NaCl solutions. Bottom plots: NaI solutions.

peptide increases slightly when salt is present. We speculate that this result is related to the enhanced ion—water interaction in the region beyond the first solvation shell, discussed with reference to Table 4 below.

The ion—water rdf's are shown in Figure S2 of the SI. The water oxygen—sodium ion rdf and the water hydrogen—anion rdf are largely insensitive to salt concentration and type. The important feature of these plots is that the contact peak is much higher than unity, in contrast to the results of Figure 10. It is clear therefore that water prefers to interact with the ions rather than with the peptide groups.

To obtain further insights on the factors contributing to the tetrapeptide conformational preferences, we split the simulation system into peptide ("P"), ion ("I"), and water ("W") components. We computed total interaction energies among all possible combinations of component pairs. These energies were averaged separately for (a) "closed" peptide conformations (with an $i/i+4$ hydrogen bond), and (b) completely extended conformations (without any intramolecular hydrogen bonds). A comprehensive list of the resulting average energies is included in Table S3 of the SI. Selected terms are reported in Table 3.

The present analysis aims to investigate whether certain energy terms decrease with salt concentration, in the presence of helical conformations, in accordance with the observed increase in the tetrapeptide helicity (Table 2). It should be noted that the observed impact of salt on helicity is small, corresponding to a sub-kcal/mol decrease in the free energy of the helical conformations. On the other

Table 3. Average Intermolecular Energies (in kcal/mol) between All Important Components of the Tetrapeptide Salt Solutions, for Closed and Extended Conformations

solution	total	energy components ^a										
		E_{PP}	E_{PW}	E_{PI}	E_{IW}	E_{II}	E_{WW}	$E_{PP}+E_{PW}+E_{PI}$	$E_{PI}+E_{IW}+E_{II}$	$E_{WW}+E_{WI}$	$E_{WI}+E_{II}$	$E_{WW}+E_{WI}+E_{II}$
Pure Water												
closed ^b	-10385	45	-95				-10335	-50		-10335		
extended ^b	-10391	50	-100				-10341	-50		-10441		
difference	-6	+5	-5				-6	0		-6		
1 M NaI												
closed	-14070	45	-82	-16	-6021	-432	-7564	-53	-6469	-13585	-6453	-14017
extended	-14066	50	-87	-16	-6028	-428	-7557	-53	-6472	-13585	-6456	-14013
difference	+4	+5	-5	0	-7	+4	+7	0	-3	0	-3	+4
1 M NaCl												
closed	-14422	45	-85	-12	-5956	-773	-7641	-52	-6741	-13597	-6729	-14370
extended	-14418	50	-90	-11	-5934	-783	-7650	-51	-6728	-13584	-6717	-14367
difference	+4	+5	-5	+1	+18	-10	-9	+1	+13	+13	+12	+3
2 M NaI												
closed	-17677	45	-69	-31	-10554	-1627	-5441	-55	-12212	-15995	-12181	-17722
extended	-17684	50	-75	-30	-10578	-1618	-5433	-55	-12226	-16011	-12196	-17629
difference	-7	+5	-6	+1	-24	+9	+8	0	-14	-16	-15	-7
2 M NaCl												
closed	-18381	45	-77	-21	-9678	-2693	-5957	-53	-12392	-15635	-12371	-18328
extended	-18384	50	-82	-21	-9680	-2695	-5957	-53	-12395	-15637	-12374	-18331
difference	-3	+5	-5	0	-2	-2	0	0	-3	-2	-3	-3
3 M NaI												
closed	-20278	45	-60	-42	-12985	-2940	-4296	-57	-15967	-17281	-15925	-20221
extended	-20282	51	-65	-43	-13038	-2915	-4272	-57	-15996	-17310	-15953	-20225
difference	-4	+6	-5	-1	-53	+25	+24	0	-29	-29	-28	-4
3 M NaCl												
closed	-21219	45	-74	-25	-11291	-4651	-5223	-54	-15967	-16514	-15942	-21165
extended	-21234	50	-77	-27	-11358	-4623	-5199	-54	-16008	-16557	-15981	-21180
difference	-15	+5	-3	-2	-67	+28	+24	0	-41	-43	-39	-15

^a“P”, “I” and “W” denote, respectively, peptide, ion, and water terms; for example, E_{PP} is the total intramolecular peptide energy; E_{IP} is the total ion–peptide energy. ^bEntries “closed” and “extended” denote tetrapeptide conformations with an $i/i+4$ hydrogen bond, or without any intramolecular hydrogen bond.

hand, the changes in various energetic averages [among helical (“closed”) and extended conformations], reported in Table 3, are on the order of 10^1 – 10^2 kcal/mol. Thus, it is difficult to attribute the helicity enhancement to a specific energy term. Furthermore, this analysis strongly emphasizes energy, while it can be argued that entropy considerations are equally important. As we explain below, our results suggest that entropic contributions are also important, even though they are not analyzed here in detail.

For each solution, the table separately reports component energies, averaged over snapshots with “closed” (helical) conformations of the peptide, and “extended” conformations. The difference in averages (extended vs closed) is also included. Column 2 contains the total energy of the solution. Columns 3–8 contain the interactions for the various combinations of component pairs. For example, column “ E_{PP} ” contains peptide intramolecular interactions; column “ E_{II} ” contains the sum of all anion–anion, anion–cation, and cation–cation interactions. In the next several columns, we further group the interactions together.

For example, the column marked “ $E_{PP}+E_{PI}+E_{PW}$ ” contains all the interactions that involve peptide groups, and the one marked “ $E_{PI}+E_{IW}+E_{II}$ ” contains all interactions involving ions. The purpose of the above groupings is to identify consistent trends in the energy differences (values near zero, negative or positive) between extended and helical conformations, which might help interpret the peptide preferences toward the former or the latter.

The total energies are reported in the second column. In pure water, they are slightly more negative (by 6 kcal/mol) when the tetrapeptide conformation is extended, due to the E_{WW} term (see below). At low salt concentrations (1 M NaI and 1 M NaCl), they become more negative with helical conformations. This change correlates nicely with the helix stabilization due to salt, but is not consistently observed at higher concentrations: at 2 M NaI and 3 M NaCl, the energies are more negative for extended conformations (respectively, by -7 and -15 kcal/mol).

Table 4. Average Ion–Water Pair Interaction Energies (in kcal/mol) between Ions and Water in Two Regions near and Away from the Peptide (See Text)

interaction ^a	peptide conformation ^b	solution					
		3 M NaI	2 M NaI	1 M NaI	3 M NaCl	2 M NaCl	1 M NaCl
E_{IA-WA}	closed	−0.8846	−0.8969	−0.8946	−0.8596	−0.9112	−0.9139
	extended	−0.8171	−0.8369	−0.8601	−0.801	−0.8378	−0.8749
E_{IA-WB}	closed	−0.0421	−0.0497	−0.0595	−0.0419	−0.0477	−0.0582
	extended	−0.0424	−0.0493	−0.5870	−0.0408	−0.0480	−0.0575
E_{IB-WB}	closed	−0.1148	−0.1273	−0.1453	−0.0993	−0.1164	−0.1434
	extended	−0.1158	−0.1283	−0.1463	−0.1003	−0.1170	−0.1438
E_{IB-WA}	closed	−0.0329	−0.0399	−0.0488	−0.0283	−0.0349	−0.0475
	extended	−0.0336	−0.0393	−0.0479	−0.0287	−0.0347	−0.0462

^a E_{IX-WY} denotes pair interactions between ions in region X and water in region Y (X, Y = A, B); regions A and B are defined in the text. ^b Entries “closed” and “extended” denote tetrapeptide conformations with an $i/i+4$ hydrogen bond, or without any intramolecular hydrogen bond.

It can be argued that these energy differences are results of subtractions of large numbers, and therefore they are not statistically significant. It turns out that the standard deviations of energy terms, such as E_{WW} , E_{IW} , or E_{II} (as calculated from block-averaging of trajectories every 5 ns) are surprisingly small (e.g., in the 3 M NaCl system we find that $E_{WW} = -5223 \pm 10$ kcal/mol and $E_{II} = -4651 \pm 12$ kcal/mol). Some of the total energy differences between extended and helical conformations reported above are comparable to these standard deviations and therefore cannot be used to establish energetic trends; however, other energy differences are meaningful. As analyzed below, individual energy components change more consistently across solutions.

Intramolecular peptide–peptide interactions (E_{PP}) are constant across solutions, reflecting the insensitivity of helical (closed) and extended conformations to the composition of the solution. These terms stabilize the helical conformations by ~5 kcal/mol, due to the approach of the N-terminal carbonyl and C-terminal amide groups and the formation of the $i/i+4$ hydrogen bond. Peptide–water interactions (E_{PW}) become less favorable (less negative) with an increase in salt concentration and anion size. This can be attributed to a competition between peptide–water and peptide–ion interactions, which is indicated by the approximately constant value of the combined term $E_{PW} + E_{PI}$ (ca. −100 kcal/mol); despite their dependence on electrolyte type and concentration, the terms E_{PW} are consistently more negative by ~5 kcal/mol in extended conformations, due to increased exposure of the peptide groups to solvent; thus, the contributions from E_{PW} and E_{PP} cancel almost exactly in the energy difference (extended vs closed).

Ion–peptide interactions (E_{PI}) become more negative with salt concentration and anion size, in accordance with the more pronounced iodide affinities for the alanine methyl groups and sodium affinities for the peptide carbonyl group. Interestingly, these terms are not sensitive to the peptide conformation! As a result, the total sum of peptide-related energy terms ($E_{PP} + E_{PW} + E_{PI}$) is fairly constant. The remaining sum, $E_{WW} + E_{WI} + E_{II}$, is more negative for extended peptide conformations in the 2 and 3 M salt solutions. The change in this sum (extended vs closed) is dominated by the contribution from the ion–water term (E_{IW}), which is anticorrelated with the contributions from the two other terms (E_{WW} and E_{II}), and approximately twice as large in absolute value.

The above analysis shows that the total sum of peptide-related energy components ($E_{PP} + E_{PW} + E_{PI}$ sum in the ninth column) is not the determining factor for the peptide conformational properties.

This somewhat surprising result further supports our earlier conclusion, that the enhanced sodium–carbonyl interactions are not solely responsible for the changes in oligopeptide helical stabilities. In most solutions, the total energy is more negative for extended peptide conformations, mainly due to the E_{IW} term. These observations do not explain our salt-induced stabilization of helical conformations, but together suggest that entropic contributions (due to solvent, salt, and peptide) are also important determining factors; accurate computation of entropic contributions is a difficult task⁸⁸ and is outside the scope of the present article.

To probe more deeply the origin of the more negative E_{IW} values with extended peptide conformations, we partitioned the simulation box into two subregions: one region (A) containing ions and water within 5.5 Å from any peptide group, and a second region (B) containing the rest of the solution. In Table 4 we decompose the total E_{IW} term into four contributions E_{IA-WA} , E_{IA-WB} , E_{IB-WA} , and E_{IB-WB} ; each term E_{IX-WY} corresponds to the interactions between ions in region X and water in region Y (X, Y = A or B). For each simulation snapshot, we divided the total values by the total number of ion–water pairs; the resulting normalized values were averaged over the simulation trajectories; the final values are reported in the table.

The strongest average ion–water pair interactions are observed in region A, due to the smaller volume of this region and the reduced ion–water distances. Ion–water interactions in this region are stronger when the peptide assumes hydrogen-bonded conformations, presumably due to a reduction in the solvent and ion accessibility of the peptide groups. On the contrary, in region B the ion–water pairwise interactions are slightly more negative for extended peptide conformations. Since the number of ion–water pairs in region B is orders of magnitude higher than that in region A, the total energy term E_{IW} slightly favors the extended conformations (as is indeed observed in the simulations), but less so in the presence of salts. In conclusion, the more negative E_{IW} values of Table 3 are due to improved ion–water interactions *outside* the peptide first hydration shell.

4. CONCLUSIONS AND PERSPECTIVE

In our investigation of salt effects on the conformations of an alanine dipeptide, we found that the “intrinsic” conformational states of the backbone, as described by Ramachandran maps, are not greatly affected even by large concentrations of NaCl and NaI. Apparently, the intrinsic tendencies of the backbone in such

a small molecule are too strong to be affected by environmental factors, a fact also mentioned by Feig.³⁹ In the case of an alanine tetrapeptide, however, the Ramachandran maps show an increased tendency for more compact conformations in the presence of salts. Cl⁻ ions prefer to stay away from the peptides, while I⁻ ions have a preferential interaction with the hydrophobic methyl groups. This preference is not a result of enhanced pairwise methyl–iodide with respect to water–iodide interactions, as is revealed in Table S2, hence it must be of entropic origin. Na⁺ ions on the other hand have a significant affinity for the carbonyl groups with a strong enthalpic component (see Table S2), a fact observed in several other recent investigations as well.^{27–31}

The tetrapeptide simulations were quite insightful, since they allowed the examination of the salt effect on the tendency for adoption of compact conformations. The helicity is enhanced in the presence of salts, with NaI being more effective. This tendency decreases with increasing temperature, as found experimentally⁸⁹ and computationally⁶³ in related systems. Our finding that helicity is enhanced by salts was associated here with a concomitant increase in the formation probabilities of the α -helical hydrogen bond ($i/i+4$), and other hydrogen bonds ($i/i+3$, $i/i+2$). It was corroborated by examining slightly longer peptides with the AMBER force-field.⁶⁴ It is thus not a force-field artifact. At first glance, this finding appears to disagree with the results of Dzubiella,²⁹ who found that salts lead to a significant decrease of helicity of a dodecapeptide. However, it must be stressed that helicity is defined in a very narrow way for a short tetrapeptide, since there is only the possibility for a single “turn” and the formation of a terminal H-bond. In addition, Dzubiella used oligopeptides containing charged residues. In further work in progress using the AMBER force-field,⁶⁴ we were able to show that much longer peptides, comparable to those of Dzubiella,^{29,30} or of Asciutto et al.,³¹ do in fact behave in an opposite way: they show decreased helicity in the presence of electrolytes. Since we believe that this major finding is robust and force-field independent, we have tried to understand its origin by a detailed energy analysis for all possible interactions in our systems. We were able to show that the enhanced helicity is not due to stronger ion–peptide interaction, or to a difference in the hydration of the peptide in the presence of ions. The detailed analysis in Tables 3 and 4 points out that the stabilization of helical conformations coexists with enhanced ion–water interactions outside the first hydration shell of the peptide. This intriguing finding in turn suggests that the stabilization may have a significant entropic component. It is interesting to examine whether this tendency of stabilization of the primary helical fold in the presence of electrolytes still holds for larger peptides. This is the focus of ongoing work, which will be presented in a subsequent paper.

■ ASSOCIATED CONTENT

S Supporting Information. The SI contains a diagram of the helicity of the investigated systems as a function of temperature. It also contains the ion–water rdf, a table containing the results of cluster analysis of the tetrapeptide conformations in various solutions, a table with average pair interactions energies between ions water and various peptide groups, and a more detailed form of the large Table 3 of the manuscript. This material is available free of charge via the Internet at <http://pubs.acs.org>.

■ AUTHOR INFORMATION

Corresponding Author

*E-mail: archonti@ucy.ac.cy (G.A.); psleon@ucy.ac.cy (E.L.).

■ ACKNOWLEDGMENT

G.A. and P.I. would like to thank the Cyprus Research Promotion Foundation and the European Union Structural Funds for financial support (project RPF/PENEK/ENISX/0308/24) during the time that this work was carried out. Most simulations were carried out in Biophysics clusters at the University of Cyprus. Some simulations were carried out at an IBM cluster of the Cyprus Institute.

■ REFERENCES

- (1) Collins, K. D.; Washabaugh, M. W. *Q. Rev. Biophys.* **1985**, *18*, 323–422.
- (2) Cacace, M. G.; Landau, E. M.; Ramsden, J. J. *Q. Rev. Biophys.* **1997**, *30*, 241–277.
- (3) Baldwin, R. L. *Biophys. J.* **1996**, *71*, 2056–2063.
- (4) Ninham, B. W.; Yaminski, V. *Langmuir* **1997**, *13*, 2097–2108.
- (5) Kunz, W., Ed. *Specific Ion Effects*; World Scientific: Singapore, 2010.
- (6) Anisimov, V. M.; Lamoureux, G.; Vorobyov, I. V.; Huang, N.; Roux, B.; Mackerell, A. D. *J. Chem. Theory Comput.* **2005**, *1*, 153–168.
- (7) Borodin, O. *J. Phys. Chem. B* **2009**, *113*, 11463–11478.
- (8) Horinek, D.; Herz, A.; Vrbka, L.; Sedlmeier, F.; Mamatkulov, S. I.; Netz, R. R. *Chem. Phys. Lett.* **2009**, *479*, 173–183.
- (9) Jungwirth, P.; Tobias, D. J. *Chem. Rev.* **2006**, *106*, 1259–1281.
- (10) Gopalakrishnan, S.; Liu, D.; Allen, H. C.; Kuo, M.; Shultz, M. J. *Chem. Rev.* **2006**, *106*, 1155–1175.
- (11) Jungwirth, P.; Tobias, D. J. *J. Phys. Chem. B* **2002**, *106*, 6361–6373.
- (12) Dang, L. X.; Chang, T.-M. *J. Phys. Chem. B* **2002**, *106*, 235–238.
- (13) Archontis, G.; Leontidis, E.; Andreou, G. *J. Phys. Chem. B* **2005**, *109*, 17957–17966.
- (14) Archontis, G.; Leontidis, E. *Chem. Phys. Lett.* **2006**, *420*, 199–203.
- (15) Schwierz, N.; Horinek, D.; Netz, R. R. *Langmuir* **2010**, *26*, 7370–7379.
- (16) Vácha, R.; Jurkiewicz, P.; Petrov, M.; Berkowitz, M. L.; Böckmann, R. A.; Barucha-Kraszewska, J.; Hof, M.; Jungwirth, P. *J. Phys. Chem. B* **2010**, *114*, 9504–9509.
- (17) Pegram, L. M.; Record, M. T. *J. Phys. Chem. B* **2008**, *112*, 9428–9436.
- (18) Lund, M.; Vrbka, L.; Jungwirth, P. *J. Am. Chem. Soc.* **2008**, *130*, 11582–11583.
- (19) Shimizu, S.; McLaren, W. L.; Matubayasi, N. *J. Chem. Phys.* **2004**, *124*, 234905.
- (20) Shulgin, I. L.; Ruckenstein, E. *Biophys. Chem.* **2005**, *118*, 128–134.
- (21) Boström, M.; Tavares, F. W.; Ninham, B. W.; Prausnitz, J. M. *J. Phys. Chem. B* **2006**, *110*, 24757–24760.
- (22) Scholtz, J. M.; York, E. J.; Stewart, J. M.; Baldwin, R. L. *J. Am. Chem. Soc.* **1991**, *113*, 5102–5104.
- (23) Smith, J. S.; Scholtz, J. M. *Biochemistry* **1998**, *37*, 33–40.
- (24) Maison, W.; Kennedy, R. J.; Kemp, D. S. *Angew. Chem., Int. Ed.* **2001**, *40*, 3819–3821.
- (25) Graf, J.; Nguyen, P. H.; Stock, G.; Schwalbe, H. *J. Am. Chem. Soc.* **2007**, *129*, 1179–1189.
- (26) Xiong, K.; Asciutto, E. K.; Madura, J. D.; Asher, S. A. *Biochemistry* **2009**, *48*, 10818–10826.
- (27) Fedorov, M. V.; Goodman, J. M.; Schumm, S. *Phys. Chem. Chem. Phys.* **2007**, *9*, 5423–5435.

- (28) Fedorov, M. V.; Goodman, J. M.; Kolombet, V. V.; Schumm, S.; Socorro, I. M. *J. Mol. Liq.* **2009**, *147*, 117–123.
- (29) Dzubiella, J. *J. Am. Chem. Soc.* **2008**, *130*, 14000–14007.
- (30) Dzubiella, J. *J. Phys. Chem. B* **2009**, *113*, 16689–16694.
- (31) Asciutto, E. K.; General, I. J.; Xiong, K.; Asher, S. A.; Madura, J. D. *Biophys. J.* **2010**, *98*, 186–196.
- (32) Heyda, J.; Vincent, J. C.; Tobias, D. J.; Dzubiella, J.; Jungwirth, P. *J. Phys. Chem. B* **2010**, *114*, 1213–1220.
- (33) Von Hansen, Y.; Kalcher, I.; Dzubiella, J. *J. Phys. Chem. B* **2010**, *114*, 13815–13822.
- (34) Yu, H.; Mazzanti, C. L.; Whitfield, T. W.; Koeppe, R. E., II; Andersen, O. S.; Roux, B. *J. Am. Chem. Soc.* **2010**, *132*, 10847–10856.
- (35) Cantor, C. R.; Schimmel, P. R. *Biophysical Chemistry*; W. H. Freeman: San Francisco, 1980; Part I.
- (36) Creighton, T. E. *Proteins: Structures and Molecular Properties*, 2nd ed.; W. H. Freeman: San Francisco, 1992.
- (37) Mu, Y.; Kosov, D. S.; Stock, G. *J. Phys. Chem. B* **2003**, *107*, 5064–5073.
- (38) Ohkubo, Y. Z.; Brooks, C. L., III. *Proc. Natl. Acad. Sci. U.S.A.* **2003**, *100*, 13916–13921.
- (39) Feig, M. *J. Chem. Theory Comput.* **2008**, *4*, 1555–1564.
- (40) Nandi, P. K.; Robinson, D. R. *J. Am. Chem. Soc.* **1972**, *94*, 1299–1308.
- (41) Hamabata, A.; von Hippel, P. H. *Biochemistry* **1973**, *12*, 1264–1271.
- (42) Collins, K. D. *Proc. Natl. Acad. Sci. U.S.A.* **1995**, *92*, 5553–5557.
- (43) Collins, K. D. *Methods* **2004**, *34*, 300–311.
- (44) Vrbka, L.; Jungwirth, P.; Bauduin, P. *J. Phys. Chem. B* **2006**, *110*, 7036–7043.
- (45) Cho, Y.; Zhang, Y.; Christensen, T.; Sagle, L. B.; Chilkoti, A.; Cremer, P. S. *J. Phys. Chem. B* **2008**, *112*, 13765–13771.
- (46) Pegram, L. M.; Record, M. T. *J. Phys. Chem. B* **2008**, *112*, 9428–9436.
- (47) Leontidis, E.; Aroti, A. *J. Phys. Chem. B* **2009**, *113*, 1460–1467.
- (48) Zangi, R. *J. Phys. Chem. B* **2010**, *114*, 643–650.
- (49) Rossky, P. J.; Karplus, M. *J. Am. Chem. Soc.* **1979**, *101*, 1913–1937.
- (50) Mezei, M.; Mehrotra, P. K.; Beveridge, D. L. *J. Am. Chem. Soc.* **1985**, *107*, 2239–2245.
- (51) Tobias, D. J.; Brooks, C. L. *J. Phys. Chem.* **1992**, *96*, 3864–3870.
- (52) Ishizuka, R.; Huber, G. A.; McCammon, J. A. *J. Phys. Chem. Lett.* **2010**, *1*, 2279–2283.
- (53) Tobias, D. J.; Brooks, C. L. *Biochemistry* **1991**, *30*, 6059–6070.
- (54) Mackerell, A. D. *J. Comput. Chem.* **2004**, *25*, 1584–1604.
- (55) García, A. E.; Sanbonmatsu, K. Y. *Proc. Natl. Acad. Sci. U.S.A.* **2002**, *99*, 2782–2787.
- (56) Buchete, N.-V.; Hummer, G. *Phys. Rev. E* **2008**, *77*, 030903(R)1–4.
- (57) MacKerrell, A. D., Jr.; Bashford, D.; Bellott, M.; Dunbrack, R. L.; Evanseck, J. D.; M. J. Field, M. J.; Fischer, S.; Gao, J.; H.; Guo, H.; Ha, S.; Joseph-McCarthy, D.; Kuchnir, L.; Kuczera, K.; Lau, F. K. T.; Mattos, C.; Michnick, S.; Ngo, T.; Nguyen, D. T.; Prodhom, B.; Reiher, W. E.; Roux, B.; Schlenkrich, M.; Smith, J. C.; Stote, R.; Straub, J.; Watanabe, M.; Wiorkevicz-Kuczera, J.; Yin, D.; Karplus, M. *J. Phys. Chem. B* **1988**, *102*, 3586–3616.
- (58) Mackerell, A. D.; Feig, M.; Brooks, C. L., III. *J. Comput. Chem.* **2004**, *25*, 1400–1415.
- (59) Mackerell, A. D.; Feig, M.; Brooks, C. L., III. *J. Am. Chem. Soc.* **2004**, *126*, 698–699.
- (60) Jorgensen, L. W.; Chandrasekhar, J.; Madura, D. J.; Impey, W. R.; Klein, L. M. *J. Chem. Phys.* **1983**, *79*, 926–93.
- (61) Neria, E.; Fischer, S.; Karplus, M. *J. Chem. Phys.* **1996**, *105*, 1902–1921.
- (62) Joung, S.; Cheatham, E. *J. Phys. Chem. B* **2008**, *112*, 9020–9041.
- (63) Best, R. B.; Buchete, N.-V.; Hummer, G. *Biophys. J.* **2008**, *95*, L07–L09.
- (64) Best, R. B.; Hummer, G. *J. Phys. Chem. B* **2009**, *113*, 9004–9015.
- (65) Verbaro, D.; Ghosh, I.; Nau, W. M.; Schweitzer-Stenner, R. *J. Phys. Chem. B* **2010**, *114*, 17201–17208.
- (66) Hegefeld, W. A.; Chen, S. E.; DeLeon, K. Y.; Kuczera, K.; Jas, G. S. *J. Phys. Chem. B* **2010**, *114*, 12391–12402.
- (67) Case, D. A.; Darden, T. A.; Cheatham, T. E. III; Simmerling, C. L.; Wang, J.; Duke, R. E.; Luo, R.; Walker, R. C.; Zhang, W.; Merz, K. M.; Roberts, B.; Wang, B.; Hayik, S.; Roitberg, A.; Seabra, G.; Kolossvari, I.; Wong, K. F.; Paesani, F.; Vanicek, J.; Liu, J.; Wu, X.; Brozell, S. R.; Steinbrecher, T.; Gohlke, H.; Cai, Q.; Ye, X.; Wang, J.; Hsieh, M.-J.; Cui, G.; Roe, D. R.; Mathews, D. H.; Seetin, M. G.; Sagui, C.; Babin, V.; Luchko, T.; Gusarov, S.; Kovalenko, A.; Kollman, P. A. *AMBER 11*; University of California: San Francisco, 2010.
- (68) Brooks, B. R.; Brooks, C. L., III; Mackerell, A. D.; Nilsson, L.; Petrella, R. J.; Roux, B.; Won, Y.; Archontis, G.; Bartels, C.; Boresch, S.; Caflisch, A.; Caves, L.; Cui, Q.; Dinner, A. R.; Feig, M.; Fischer, S.; Gao, J.; Hodoscek, M.; Im, W.; Kuczera, K.; Lazaridis, T.; Ma, J.; Ovchinnikov, V.; Paci, E.; Pastor, R. W.; Post, C. B.; Pu, J. Z.; Schaefer, M.; Tidor, B.; Venable, R. M.; Woodcock, H. L.; Wu, X.; Yang, W.; York, D. M.; Karplus, M. *J. Comput. Chem.* **2009**, *30*, 1545–1614.
- (69) Darden, T.; York, D.; Petersen, L. *J. Chem. Phys.* **1993**, *98*, 10089–10092.
- (70) Ryckaert, J. P.; Ciccotti, G.; Berendsen, H. J. C. *J. Comput. Phys.* **1977**, *23*, 327–341.
- (71) Nose, S. *J. Chem. Phys.* **1984**, *81*, 511–519.
- (72) Hoover, W. G. *Phys. Rev. A* **1985**, *31*, 1695–1697.
- (73) Lifson, S.; Roig, A. *J. Chem. Phys.* **1961**, *34*, 1963–1974.
- (74) Wilmot, C. M.; Thornton, J. M. *Protein Eng.* **1990**, *3*, 479–493.
- (75) Carpenter, G. A.; Grossberg, S. *Appl. Opt.* **1987**, *26*, 4919–4930.
- (76) Karpen, M. E.; Tobias, D. T.; Brooks, C. L. *Biochemistry* **1993**, *32*, 412–420.
- (77) Tamamis, P.; Skourtis, S.; Lambris, J. D.; Morikis, D.; Archontis, G. *J. Mol. Graphics Modell.* **2007**, *26*, 571–580.
- (78) Hu, H.; Elstner, M.; Hermans, J. *Proteins: Struct., Funct., Genet.* **2003**, *50*, 451–463.
- (79) Poon, C.-D.; Samulski, E. T. *J. Am. Chem. Soc.* **2000**, *122*, 5642–5643.
- (80) Weisse, C. F.; Weisshaar, J. C. *J. Phys. Chem. B* **2003**, *107*, 3265–3277.
- (81) Grdadolnik, J.; Grdadolnik-Golić, S.; Avbelj, F. *J. Phys. Chem. B* **2008**, *112*, 2712–2718.
- (82) Woutersen, S.; Pfister, R.; Hamm, P.; Mu, Y.; Kosov, D. S.; Stock, G. *J. Chem. Phys.* **2002**, *117*, 6833–6840.
- (83) Schweitzer-Stenner, R.; Measey, T.; Kakalis, L.; Jordan, F.; Pizzanelli, S.; Forte, C.; Griebenow, K. *Biochemistry* **2007**, *46*, 1587–1596.
- (84) Gnanakaran, S.; Garcia, A. E. *J. Phys. Chem. B* **2003**, *107*, 12555–12557.
- (85) Kaminski, G. A.; Friesner, R. A.; Tirado-Rives, J.; Jorgensen, W. L. *J. Phys. Chem. B* **2001**, *105* (28), 6474–6487.
- (86) Lindahl, E.; Hess, B.; van der Spoel, D. *J. Mol. Model.* **2001**, *7*, 306–317.
- (87) Rick, S. W. *J. Chem. Phys.* **2004**, *120*, 6085–6093.
- (88) Kuffel, A.; Zielkiewicz, J. *J. Phys. Chem. B* **2008**, *112*, 15503–15512.
- (89) Shalongo, W.; Dugad, L.; Stellwagen, E. *J. Am. Chem. Soc.* **1994**, *116*, 8288–8293.